ACS Catalysis

Perspective

pubs.acs.org/acscatalysis

Direct Photocatalysis by Plasmonic Nanostructures

Matthew J. Kale,[†] Talin Avanesian,[†] and Phillip Christopher*[,†,‡]

[†]Department of Chemical & Environmental Engineering and [‡]Program in Materials Science & Engineering, University of California, Riverside, Riverside, California 92521, United States

ABSTRACT: Recent reports have shown that plasmonic nanostructures can be used to drive direct photocatalysis with visible photons, where nanostructures act as the light absorber and the catalytic active site. These reports have showcased direct plasmon driven photocatalysis as a route to concentrate and channel the energy of low intensity visible light into adsorbed molecules, enhancing the rates of chemical transformations, and offering pathways to control reaction selectivity. In this perspective, we will discuss the fundamental photophysics of localized surface plasmon resonance (LSPR) excitation in the context of driving chemical transformations. The various demonstrated chemical conversions executed using direct plasmonic photocatalysis will be reviewed. Experimental observations, such as the dependence of photocatalytic rate on illumination intensity and photon energy, will be related to microscopic mechanisms of photocatalysis. In addition, theoretical treatments of various mechanisms within the process of direct plasmonic photocatalysis will be discussed and related to experimental studies. Throughout the Perspective, the possibility of activating targeted adsorbate bonds to allow rational manipulation of reaction selectivity in direct plasmonic photocatalysis will be discussed.

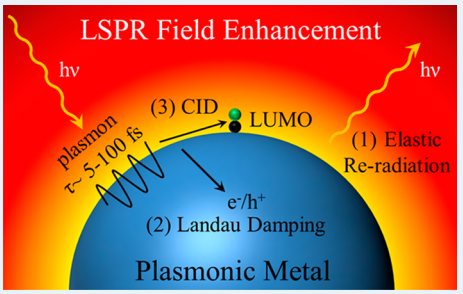

KEYWORDS: *photocatalysis, surface plasmons, selectivity, nanoparticles, solar energy*

1. INTRODUCTION AND BACKGROUND

The utilization of solar energy to drive catalytic chemical transformations on surfaces has been touted as an environmentally friendly potential alternative to traditional thermally driven heterogeneous catalysis.[1−4] The diffuse nature of sunlight, making solar photons a fairly expensive feedstock, dictates that utilizing solar energy to drive chemistry is primarily worthwhile for chemical transformations that are not attainable with thermal catalytic processes.[5] The most studied examples are endothermic reactions, such as H_2O splitting and CO_2 reduction, where the energy of solar photons can be stored in chemical bonds.[6−8] Another interesting, but scarcely demonstrated, example is the utilization of photocatalysis to manipulate and control selectivity in chemical transformations on surfaces with the end goal of executing reactions that have not been achieved via thermal catalysis.[9,10]

Thermally driven heterogeneous catalytic processes rely on manipulation of activation barriers and adsorption energies of intermediates in competing chemical pathways to control product selectivity. However, relationships inherent in nature dictate that adsorption energies of surface bound intermediates and activation barrier heights of elementary steps are related in a predictable, linear fashion.[11−13] As a result, optimization of catalytic selectivity is limited because the manipulation of energetics associated with a single elementary step will affect the energetics of other elementary steps in a predetermined manner.[14−16] Breaking down these intrinsic relationships through manipulation of energetics associated with a single elementary step without affecting the energetics of other steps has proven to be a very difficult task in heterogeneous thermal catalysis. Alternatively, photocatalysis at surfaces has the potential to allow control of single elementary step energetics, but this control hinges on the design of materials that selectively deposit the energy of photons into targeted adsorbate orbitals associated with the activation of desired chemical bonds.[10]

In this Perspective, we will discuss recent results that demonstrate the execution of photocatalysis on coinage (Ag, Au, and Cu) metal nanoparticles through the excitation of localized surface plasmon resonance (LSPR). The use of LSPR excitation to drive photocatalysis falls primarily into two categories: (a) indirect photocatalysis, where excitation of LSPR is used to transfer photon energy to nearby semiconductors,[17−20] molecular photocatalysts, and other metals[21] to drive chemistry remotely and (b) direct photocatalysis, where coinage metal nanoparticles act as the light absorber and the catalytically active site.[22] In other words, we consider direct plasmonic photocatalysis as chemical transformations that occur on the surface of plasmonic nanostructures in response to photoexcitation of LSPR on plasmonic nanostructures. This Perspective focuses on direct photocatalytic reactions driven by low-intensity (within an order of magnitude of solar intensity) visible photons on plasmonic nanoparticle surfaces. Readers should refer to previous reviews for discussions on indirect photocatalytic processes mediated by LSPR excitation.[23−25]

It is not surprising that plasmonic nanoparticles have been considered for photocatalysis, based on their well-known surface catalytic properties and strong light-matter interac-

Received: October 29, 2013
Revised: November 27, 2013
Published: December 2, 2013

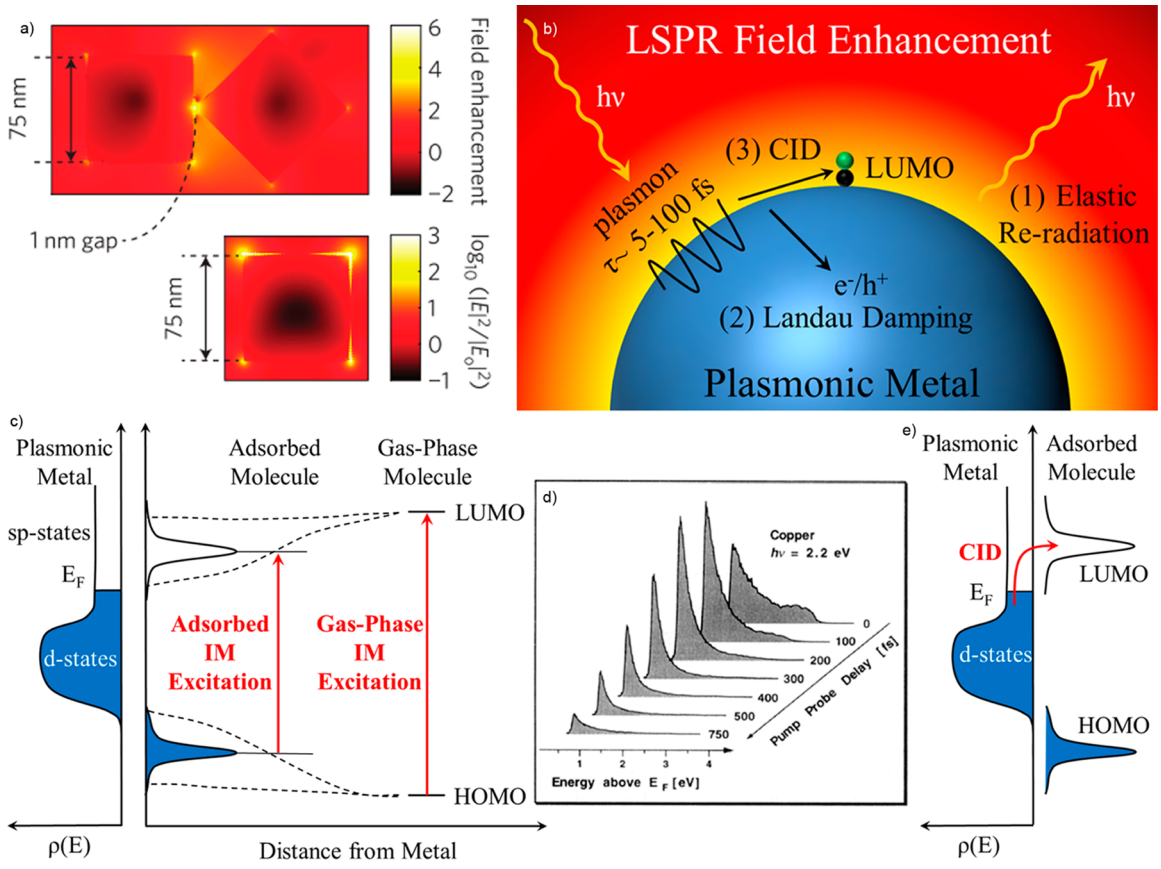

Figure 1. (a) Electric field intensity distribution calculated using the Finite Difference Time Domain (FDTD) method of an isolated 75 nm Ag nanocube (bottom), and two Ag nanocubes separated by 1 nm (top) at their respective LSPR peaks. Reproduced with permission from ref 31. Copyright 2012 Nature Publishing Group. (b) Schematic showing the three dephasing mechanisms of oscillating surface plasmons. (c) The impact of chemisorption on the HOMO−LUMO intermolecular (IM) excitation band gap of the adsorbate. (d) A series of two-photon photoemission (2PPE) spectra captured from a Cu single crystal at various delay times following a pulsed femtosecond photon excitation. This shows the evolving electron energy distribution above E_f after photon excitation. Reproduced with permission from ref 35. Copyright 1997 Elsevier Inc. (e) Proposed mechanism of direct charge injection from metal to molecular states occurring during plasmon dephasing in the CID mechanism.

tions.[22] Regardless of the strong and tunable interaction between visible light and excited plasmonic nanoparticles, direct plasmonic photocatalysis was initially regarded as improbable because of the short lifetimes of plasmon derived charge carriers and extremely fast quenching of electronically excited adsorbates on metal surfaces.[26] Against intuition that long-lived charge carriers and excited states are requisite for photocatalytic functionality, demonstrations of direct plasmon driven photocatalysis are becoming numerous, and the underlying mechanisms that allow for relatively high efficiencies in the utilization of photons to overcome activation barriers are starting to be understood.

We will begin this Perspective with a discussion of LSPR excitation and the necessary photophysics required to understand how LSPR excitation could induce direct plasmonic photocatalysis. Following this is an overview of the demonstrations of direct plasmonic photocatalysis by LSPR excitation. The remainder of the Perspective is dedicated to a critical analysis of the mechanisms associated with LSPR driven direct photocatalysis, relating mechanistic details to experimental observations. The salient role of plasmon excitation in various demonstrated model reactions will be highlighted, and the potential for driving selective chemical reactions via LSPR excitation will pervade the discussions. We will conclude with an outlook on the direction this field is moving and a discussion of the unanswered questions that have been raised.

2. LOCALIZED SURFACE PLASMON RESONANCE

Our discussion on LSPR excitation is from a dynamical, temporally evolving point of view. We feel that this allows a better understanding of the potential energy exchange between plasmon derived energetic charge carriers and adsorbates. The excitation of LSPR occurs when a nanostructured material with high free electron mobility (Ag, Au, Cu, Al, doped semiconductors, etc.) interacts with photons that match the resonance energy of the oscillation of surface valence electrons against the restoring force of the positively charged surface nuclei.[27,28] In the case of Ag, Au, and Cu this resonance energy occurs in the visible regime. The interaction of resonant photons and surface electrons initially results in the coherent oscillation of electrons in space and energy. This leads to the confinement of photon energy to the surface of nanostructured materials for much longer time scales than photons would spend in the same control volume traveling at the speed of light. As a result of this interaction, the very high absorption coefficient of photons in resonance with plasmon excitation and capacitive coupling between clusters of plasmonic particles, LSPR excitation produces a large buildup of photon intensity (strong electric fields) and a high concentration of energetic

dx.doi.org/10.1021/cs400993w | ACS Catal. 2014, 4, 116−128

electrons at nanostructured surfaces.[27,29,30] For example, resonant photon excitation of isolated cubic shaped Ag nanoparticles can enhance incoming light intensity up to 10^3 fold at certain areas on the nanoparticle surface, and junctions between Ag particles can enhance the light intensity by up to 10^6 times, see Figure 1a.[31] The lifetime of the coherent electron oscillation due to a plasmon excitation is ∼5−100 fs,[32] and can dephase through three mechanisms, (1) elastic radiative re-emission of photons, (2) nonradiative Landau damping, resulting in the excitation of energetic electrons and holes in the metal particle, and (3) the interaction of excited surface plasmons with unpopulated adsorbate acceptor states, inducing direct electron injection into the adsorbate acceptor states, called chemical interface damping (CID), see Figure 1b.[33,34] The magnitude of field enhancement, resonant wavelength, and fraction of plasmon excitations decaying through mechanisms (1)−(3) is a function of nanostructure geometry, composition, and local environment.[27,29]

All three plasmon decay processes can deposit energy into adsorbates, although they have different mechanisms. In this section we will discuss mechanisms of energy transfer from excited surface plasmons to adsorbates and will describe how the energy transfer can result in photocatalytic reactions later in the Perspective. In the radiative plasmon decay process, (1), adsorbed molecules can gain energy through the absorption of photons from intense, reradiated photon fluxes from the plasmonic nanostructure. Energy gain through this mechanism is most commonly seen when adsorbates have an intramolecular, allowable electronic transition with energy of similar magnitude to the energy of reradiated photons. If this condition is met, vibrational energy can be gained by the adsorbate through photon absorption induced vibronic energy exchange, typically discussed in the context of the Franck−Condon Principle.[36] In this case, the plasmonic metal nanostructure acts to modify the energy of the internal molecular electronic transition of a molecule, compared to the molecule's gas phase gap between the highest occupied molecular orbital (HOMO) and the lowest unoccupied molecular orbital (LUMO), through chemical bonding to the nanostructure surface, see Figure 1c. This type of photochemical process has been observed for small molecule activation at nonplasmonic metal surfaces, but a commonality of these cases is the requirement of UV photons to excite the internal electronic transition in the adsorbate.[36] It is worth mentioning that this mechanism is analogous to the well-known electromagnetic enhancement mechanism in surface-enhanced Raman spectroscopy (SERS). Although, in SERS, photon interaction with the adsorbate polarizes electrons along the axis of a chemical bond by exciting electrons to virtual states, rather than well-defined states associated with allowable electronic transitions.[37] The electromagnetic SERS excitation mechanism is less likely to induce chemical reactions compared to adsorbate photon absorption via allowable electronic transitions and also requires the bond to be polarizable. Although we caution that photon absorption by adsorbed molecules should be considered when analyzing mechanisms of surface mediated photocatalytic processes, particularly with large dye-like molecules that have electronic transitions in the visible regime, we will not focus on these processes because of our interest in visible photon driven photocatalysis with small molecules.

Energy exchange to adsorbates by plasmon decay process (2) can occur via transient transfer of plasmon derived energetic charge carriers, energetic electrons (holes), between metal nanoparticle surfaces and unpopulated (populated) orbitals of adsorbed species. Later in the Perspective the details of the interaction between energetic charge carriers and adsorbates will be discussed; here we focus on the evolution of the system after plasmon decay via mechanism (2). In process (2), plasmons decay through Landau damping where photon energy is converted to single electron/hole pair excitations, occurring ∼10 fs after initial plasmon excitation.[34] The single electronic excitations will occur from below the metal Fermi level energy, E_f, to above E_f creating a constant probability distribution of finding primary excited electrons at energies between E_f and $E_f + h\nu$. The probability distribution is relatively constant because Landau damping occurs as intraband transitions between states of sp character that have constant density a few eV above and below E_f in coinage metals.[38]

The excited primary electrons interact with other electrons through Coulombic inelastic scattering, where a cascading process spreads the energy of the primary electron across many electrons. Electrons and holes created in metals are not intrinsically correlated as they are in semiconductors and as a result, energy relaxation via electron/hole pair recombination is minimal. During the first few hundred fs the distribution of electron energies is considered to be "athermal", because it does not follow the thermal Fermi−Dirac distribution.[39,40] Through this cascading electron energy exchange process the distribution of electron energies in the nanostructure evolves temporally. Experimentally, the temporally evolving energetic electron distribution above E_f has been measured using spectroscopic techniques, such as time-resolved two-photon photoemission spectroscopy (2PPE).[41] A variation of the femtosecond laser pump and probe pulse time delays in 2PPE reveal snapshots of the evolution of electron energies at given time steps, see Figure 1d.[35] The evolution of energetic electron distribution after plasmon dephasing is important for understanding the time scale of energy transfer from energetic electrons to adsorbates via transient charge transfer.

In parallel with the cascading process of electron energy spreading, low energy electrons couple to phonon modes thereby heating up the metal lattice with a time scale of ∼1 ps, followed by the dissipation of this heat to the surrounding environment in a time scale of 10−100 ps.[40,42] Plasmon mediated nanostructure heating could result in energy transfer to adsorbates, which would drive chemical transformations through an Arrhenius dependence of rate on surface temperature. Experimental and theoretical analyses of plasmon mediated nanostructure heating have shown that under illumination of solar intensity (100 mW/cm^2), maximum transient temperature increases of only ∼10^{-2} K can be achieved.[43,44] Assuming that the rate of a thermal reaction doubles with a 10 K increase in operating temperature (apparent activation barrier of ∼100 kJ/mol), an illumination intensity of 10^6 mW/cm^2 would be necessary to produce a 2-fold increase in the rate of reaction due to plasmonic heating. Although, the plasmonic heating mechanism should be considered when analyzing photocatalytic reaction mechanisms on illuminated plasmonic particles, under low intensity illumination this mechanism most likely does not play a role in inducing chemistry, particularly when reactions are run in continuous-flow, isothermal environments.

The first two plasmon decay mechanisms occur regardless of environmental conditions, but the addition of adsorbates to the surface of plasmonic nanostructures can induce a new, ultrafast dephasing pathway, occurring on the scale of ∼5 fs, through

dx.doi.org/10.1021/cs400993w | ACS Catal. 2014, 4, 116−128

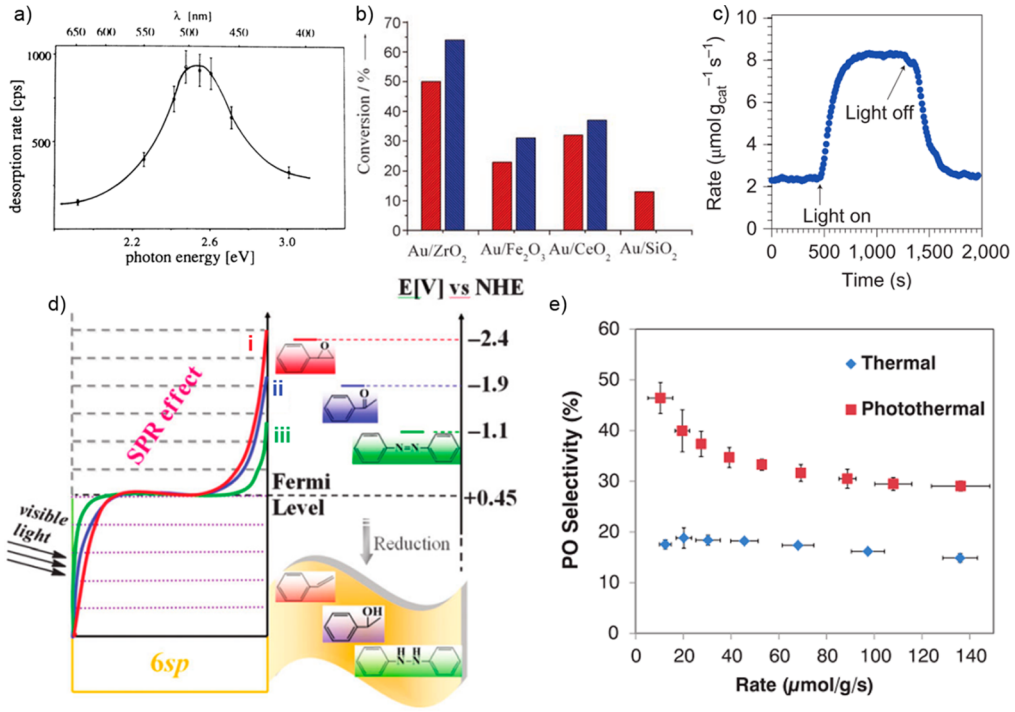

Figure 2. (a) The dependence of Na desorption rate from 50 nm Na clusters on the photon excitation wavelength (energy). Reproduced with permission from ref 57. Copyright 1988 American Physical Society. (b) Magnitude of HCHO conversion to CO_2 measured under blue light (blue bars) and red light (red bars) for Au nanoparticle catalysts on various oxide supports. Reproduced with permission from ref 60. Copyright 2008 Wiley-VCH. (c) The rate of ethylene oxide formation via the ethylene epoxidation reaction measured at 450 K with 250 mW/cm^2 visible illumination, and without illumination. Reproduced with permission from ref 43. Copyright 2011 Nature Publishing Group. (d) (Left) Proposed Electronic band structure of supported Au nanoparticles under different color illuminations: (i) 420 nm, (ii) 550 nm, and (iii) 600 nm. (Right) Overlap of the Au band structure with the reduction potentials for various reduction reactions. Modified from ref 65. Copyright 2012 Royal Society of Chemistry. (e) Thermal (dark) and photothermal (under illumination) selectivity of propylene epoxidation to propylene oxide as a function of reaction rate. Reproduced with permission from ref 9. Copyright 2013 American Association for the Advancement of Science.

CID (3).[45−47] The interaction of coherently oscillating plasmons with unpopulated electronic states of adsorbates has been shown to induce dephasing through the direct transfer of energetic charge carriers to unpopulated adsorbate states, see Figure 1e. CID is thought to be similar in a microscopic picture to the interaction of energetic electrons produced through Landau damping with adsorbates, with the main differences being the time scales of the processes, the coherent nature of the energy transfer process, and potentially the resonant wavelength dependent energy transfer efficiency. Atomic scale insights into the electronic and energetic exchange processes involved in CID are still being developed, although recent advances in time dependent density functional theory (TDDFT) are beginning to answer some of these questions.[48]

The main difference between LSPR mediated electronic energy transfer to adsorbates via processes (2) and (3) is whether energetic electrons are initially generated in the metal due to Landau damping and subsequently scatter into adsorbate states, (2), or energetic electrons are directly injected into adsorbate states at the instant of plasmon dephasing, (3). The physical manifestation of this distinction is that adsorbates may experience a large difference in electron energy distribution depending on whether the energy transfer occurs directly, or some time after dephasing. As a result of the temporally evolving electron energy distribution in process (2), photocatalytic reactions induced through processes (2) and (3) may display very different photocatalytic efficiencies and mechanistic characteristics.

Based on our analysis of the viability of potential plasmon induced photocatalytic mechanisms, the remainder of this Perspective will focus on the ability of energetic electrons (either directly transferred to adsorbates, or generated within the metal structure followed by transfer to the adsorbates) produced through Landau damping to drive photocatalysis through low intensity visible light excitation. In the next section we provide an overview of the reports of plasmon driven photocatalysis, followed by a detailed discussion of their mechanistic characteristics.

3. OBSERVATIONS OF PLASMON DRIVEN PHOTOCATALYSIS ON METALLIC NANOPARTICLES

Photon mediated, electron driven chemical transformations on metal surfaces have been studied in detail for the past 40 years. Until recently, heterogeneous photocatalysis on metal surfaces has primarily involved the execution of single elementary steps (desorption or dissociation) occurring on metal single crystals induced by intense laser irradiation.[49−51] The fundamental physics governing the interaction of energetic electrons in single crystals and adsorbates provides much of the physical framework for understanding direct plasmon driven photocatalysis. These studies have identified crucial mechanistic characteristics of electron driven processes at metal surfaces and have shown conclusively that energetic electrons can execute reaction pathways that thermal energy cannot.[10] But, it has also been shown that extended structures are highly inefficient photocatalytic materials.[33] Our interest in direct plasmon

dx.doi.org/10.1021/cs400993w | ACS Catal. 2014, 4, 116−128

driven photocatalysis is motivated by the opportunity to control reaction selectivity and the potential for performing these chemistries with high efficiencies under solar irradiation.

The majority of research studying plasmonic nanoparticles interacting with adsorbates has focused on SERS, where plasmon-induced local field enhancements cause significant enhancements in Raman signals from molecules near nanostructured noble metal surfaces. Indirect evidence of electron driven catalytic reactions mediated by LSPR excitation comes from reports of bond scission induced by plasmonic excitation during SERS experiments.[52−54] It was seen that molecules examined via SERS would exhibit unexpected vibrational signatures, which were attributed to the well-known "chemical-enhancement mechanism".[55] In addition, it was noted that Raman signals of molecules on Ag and Au surfaces would change during Raman experiments, indicating that some chemical transformation occurred. The mechanism of these unexpected results remains a topic of significant interest, but ties between SERS experiments and plasmon driven photocatalysis are providing important mechanistic insights. It is also worth noting that theoretical descriptions of the "chemical enhancement" mechanism in SERS are similar to models for electron driven reactions developed by the surface science community and those discussed in this Perspective.[56]

The first convincing evidence of a plasmon mediated, electron driven chemical process was reported in 1988 based on visible photon-induced desorption of Na atoms from 50 nm Na particles deposited on optically transparent LiF substrates.[57] The rate of Na desorption as a function of photon wavelength was similar to the wavelength dependent LSPR spectrum of the Na clusters providing evidence that Na desorption was due to plasmon excitation of the Na clusters, see Figure 2a. Furthermore, the authors state that the intensity of the visible light and the low energy of the photons preclude any thermally induced Na desorption or Na ionization, indicating that the process was electron-driven.[57] Other reports of low intensity, photon driven molecular desorption from roughened Ag surfaces and Ag nanoparticles mediated by LSPR have been published, providing a solid foundation for the execution of direct photocatalytic reactions on plasmonic nanostructures.[58,59]

The first report of a complete catalytic cycle executed due to low intensity visible light excitation of a plasmonic nanostructure on a nonphotoactive support (a support that cannot be electronically excited with the incident photon energy used in the experiments) came in 2008.[60] It was shown that Au nanoparticles supported on optically inert SiO_2 were active under red light illumination (600−700 nm) for HCHO oxidation to CO_2 at ambient temperatures. Figure 2b shows the conversion of HCHO over a series of Au based photocatalysts under blue or red light illumination. Although the figure shows results of photocatalysis with Au nanoparticles on visible light active semiconductors (Fe_2O_3), the photocatalytic activity of Au on SiO_2 clearly demonstrated that Au nanostructures on optically inactive supports could induce chemical reactions through direct plasmonic photocatalysis. The photocatalytic activity was attributed to a plasmonic heating effect, but in subsequent papers the group considered the effect to be electronic in nature.[61] The same group followed this initial publication with a series of other reports showing the unique properties of Ag and Au (on supports that cannot absorb visible light) for driving reactions at room temperature, such as sulforhodamine-B oxidation on Au and Ag,[62] selective reduction of various organics and nitroaromatics on Au,[63] and hydroamination of alkynes on Au.[64]

Our own initial report, concurrent with those above, showed that the rate of ethylene epoxidation ($C_2H_4 + 1/2O_2 \rightarrow C_2H_4O$) executed over Ag nanocubes supported on Al_2O_3 could be significantly enhanced due to low intensity visible light illumination.[43] This work showed that production rate of ethylene oxide at 200 °C in the dark, was identical to that of a catalyst operating at 160 °C under 250 mW/cm^2 visible illumination (∼2−3 suns), indicating that the plasmonic activity of the Ag catalysts allowed a unique route toward enhancing the energy efficiency of important selective chemical reactions, see Figure 2c. It was also shown that the rates of CO oxidation and NH_3 oxidation by O_2 over the Ag nanocube catalyst were significantly enhanced due to visible light illumination of the catalyst. The mechanistic details will be discussed later, but it is worth mentioning that this was the first report to show convincing evidence that the direct plasmon driven catalytic cycle was electronic in nature. Over the past few years there have been a number of other reports of direct plasmon driven photocatalysis including the unique coupling of an aldehyde, amine, and phenylacetylene to produce proparglyamines over Au surfaces,[66] photo-Fenton reactions on Au,[67] 9-anthraldehyde oxidation by Au,[68] N−N bond formation to produce *p,p′*-dimercaptoazobenzene,[69] methylene blue decomposition,[70] Suzuki coupling,[71] among others.[53,72,73] A commonality among all of these studies is the use of low intensity visible photons to execute chemical reactions on the plasmonic surface, although the level of mechanistic analysis varies significantly in each report.

A majority of the direct plasmonic photocatalysis reports show that the excitation of LSPR on catalytically active plasmonic nanoparticles acts to enhance the rate of a particular reaction compared to the rate in the dark, basically a photoassisted catalytic reaction. In a few cases it has been shown that the plasmon driven chemical processes display unique selectivity compared to pure thermal counterparts. For example, Zhu et al. showed that in the visible light driven reduction of nitrobenzene on Au nanoparticles, azobenzene could be produced whereas in a pure thermal process, nitrobenzene was over reduced to form aniline.[63] It was suggested that the low temperature operating conditions allowed by the plasmon-enhanced catalysis enabled the unique selectivity. Another approach to controlling selectivity recently demonstrated by Ke and co-workers showed that there was a relationship between the reduction potential of organic molecules and the required photon energy to drive the reactions.[65] Molecules with high reduction potentials required higher energy photons to induce the reactions, indicating a novel potential route to control selectivity, see Figure 2d. In addition, it was shown recently by Marimuthu et al. that plasmon excitation of Cu_2O@Cu core shell nanoparticles could induce a reduction of the Cu_2O shell, thereby exposing the metallic Cu surface and significantly enhancing the selectivity in the gas phase epoxidation of propylene, see Figure 2e.[9] In each of these cases, the mechanisms of selectivity control were proposed as being induced by different physical phenomena.

The reports of direct plasmonic photocatalysis to date show conclusively that excitation of LSPR via low intensity continuous wave photon illumination can induce significant enhancement in rates of reactions that are typically performed exclusively with thermal energy. Following a simple thought process, this means that in each reaction the LSPR excitation

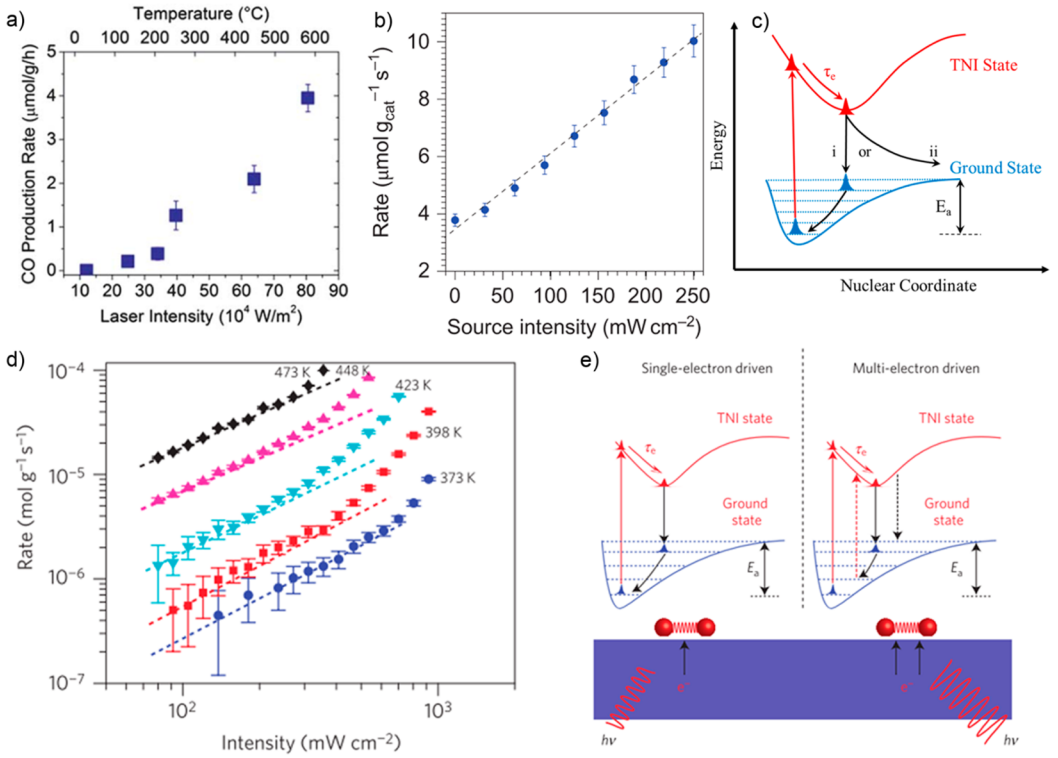

Figure 3. (a) CO production rate from a CO_2 and H_2 mixture over Au nanoparticles supported on ZnO as a function of continuous wave laser intensity (532 nm) and the calibrated steady state temperature. Reproduced with permission from ref 74. Copyright 2013 Royal Society of Chemistry. (b) The rate of photothermal ethylene oxide formation as a function of visible light intensity. Reproduced with permission from ref 43. Copyright 2011 Nature Publishing Group. (c) Schematic of the proposed mechanism for electronic excitation of adsorbed molecules through a TNI PES. This process can result in the adsorbate (i) gaining vibrational energy, or (ii) overcoming an activation barrier, inducing a chemical transformation. (d) Ethylene epoxidation photocatalytic rate measured as a function of visible light intensity for various temperatures. Reproduced with permission from ref 31. Copyright 2012 Nature Publishing Group. (e) Proposed mechanism of the linear dependence of photocatalytic rate on source intensity (left) and for the superlinear dependence of rate on source intensity through multiple electronic excitations of a single adsorbate (right). Reproduced with permission from ref 24. Copyright 2011 Nature Publishing Group.

channels photon energy to speed up the rate-limiting step. Furthermore, the few examples where catalytic selectivity was modulated by LSPR excitation provide initial evidence that direct plasmon driven photocatalysis may allow for unique routes to control catalytic selectivity. Although, significantly more insights into how LSPR excitation affects various elementary steps on surfaces will need to be developed before it can be concluded that LSPR excitation can be utilized to manipulate the energetics of a single elementary step in an overall catalytic cycle. In the next section, we will discuss a mechanistic picture of direct plasmonic photocatalysis driven by low intensity illumination that is consistent with all reports. In addition, we will discuss the effect of plasmon decay mechanism, operating temperature, and excited state potential energy surface (PES) characteristics on the efficiency of direct plasmon driven photocatalytic processes.

4. IMPACT OF ILLUMINATION INTENSITY ON DIRECT PLASMONIC PHOTOCATALYSIS

Very early in the study of heterogeneous photocatalysis on surfaces, researchers found that macroscopically observable photocatalytic rate dependence on illumination intensity provides microscopic mechanistic information.[36] Detailed intensity dependent studies of photocatalysis on metals and semiconductors have been performed under a wide range of conditions, and generally the intensity, I, dependence of photocatalytic rate falls into 4 categories: sublinear (Rate $\propto I^n$, $n < 1$), linear (Rate $\propto I$), superlinear (Rate $\propto I^n$, $n > 1$), and exponential (Rate $\propto e^{f(I)}$). Each of these dependences can be mathematically derived using rate equations of the elementary steps involved in the photocatalytic cycle, and are signatures that provide information about the mechanism of photon utilization. Direct plasmon driven photocatalysis has been observed to display each of these dependences, (except for the sublinear relationship that is only observed in semiconductor photocatalysts when bulk electron hole pair recombination is prevalent) which occur under different operating conditions. We will relate the observed intensity dependent relationships for direct plasmonic photocatalysis to experimental conditions they have been observed under, in an attempt to provide a holistic picture of the different mechanisms by which direct plasmon driven photocatalysis can be executed and the salient role of plasmon excitation in each case.

Exponential relationships between photon-induced rates of chemical transformations and illumination intensity, (Rate $\propto e^{f(I)}$), provide evidence that reactions are driven through a thermal process.[43] Heating of nanoparticles via plasmon excitation has been studied in detail, experimentally and theoretically, showing that there is a linear relationship between the change in surface temperature of plasmonic nanoparticles and the illumination intensity.[44] Coupling this linear relationship with the Arrhenius expression for thermally driven chemical reactions shows that plasmon heating induced chemistry will display an exponential dependence of rate on

dx.doi.org/10.1021/cs400993w | ACS Catal. 2014, 4, 116−128

illumination intensity. For example, a recent study of CO_2 and H_2 conversion over Au/ZnO showed an exponential dependence of CO production rate on laser intensity, which quantitatively matched expected results in a thermally driven process, see Figure 3a.[74] ZnO is a semiconductor with a band gap of ∼3.3 eV, thus visible light absorption in these experiments only occurred by the Au nanostructures. An intensity of 250 W/cm^2 was required to observe any CO_2 conversion, which is greater than 3 orders of magnitude higher intensity than average solar irradiance. In addition, the study was performed in a batch reactor with no thermal cooling. Based on the high photon flux required to drive chemistry through plasmonic heating, even in static, unregulated temperature environments, we suggest that the heating mechanism will play a minor role in observations of direct plasmonic photocatalysis under irradiation of similar intensity to the sun. Thus, even though plasmonic nanoparticles are excellent photon-induced heat generators under resonant excitation, owing to their very high absorption coefficients, it is not expected that the exponential dependence of rate on intensity will be observed with low intensity photon illumination of temperature regulated reactors. Furthermore, the utilization of the plasmon heating mechanism to drive chemistry is analogous to externally heating the system and does not provide a unique pathway to control reaction selectivity.

The most commonly reported dependence of direct plasmonic photocatalytic rate on photon intensity has been a linear relationship, (Rate $\propto I$). For example, linear relationships have been observed for ethylene epoxidation on Ag nanocubes,[43] NO desorption from Ag nanoparticles,[75] photo-Fenton reaction on Au nanoparticles,[67] H-D formation from H_2 and D_2 dissociation on Au nanoparticles,[73] among others, see Figure 3b.[43] These observations were reported for a wide range of photon intensities and catalyst geometries, making it difficult to generalize the conditions under which this behavior dominates direct plasmonic photocatalysis. We note that in the case of Au/TiO_2,[73] visible light induced energetic electron transfer from the metal to support could occur, raising the question of whether chemistry occurs on Au or on TiO_2. Linear relationships have been reported many times previously for heterogeneous photocatalysis on semiconductor and metal single crystal surfaces and are evidence of first order processes in photons. In the context of direct plasmonic photocatalysis, a first order process in visible photons suggests that each reaction is induced by a single photon absorption event followed by the interactions of the resulting electronic charge carriers and the adsorbate.

Further evidence that the linear rate dependence on intensity is associated with an electron driven process was provided by isotopic labeling experiments.[76] Isotopic labeling of reactants involved in thermally driven catalytic processes has been used to identify rate-limiting steps through measurement of the kinetic isotope effect (KIE). KIE is obtained by measuring the change in rate due to the introduction of a labeled reactant and can be theoretically predicted using transition state theory. Studies of electron driven processes at metal surfaces have shown that electron driven processes display enhanced KIEs as compared to the thermal reactions. KIE measurements were performed for ethylene epoxidation on Ag nanocubes by comparing the rate of reaction using O_2^{16} and O_2^{18} for the thermally driven reaction and the plasmon enhanced process.[43] It was seen that the KIE, Rate(O_2^{16})/Rate(O_2^{18}), for ethylene epoxidation is much larger under LSPR excitation (KIE_{LSPR} = 1.19) than the KIE of the pure thermal reaction ($KIE_{Thermal}$ = 1.06). This enhanced KIE was a clear signature that the energetic electrons, created due to plasmon excitation, were acting to facilitate the O_2 dissociation reaction (the rate limiting step in ethylene epoxidation).[49,77,78]

The proposed mechanism of first order intensity dependent LSPR mediated photocatalysis is analogous to processes of desorption induced by electronic transitions (DIET).[79] Plasmon derived charge carriers that have an energetic and spatial overlap with unpopulated adsorbate electronic states can transiently scatter through the unpopulated adsorbate states for ∼1−20 fs, see Figure 3c, creating a transient negative ion (TNI) adsorbate.[80] Once the TNI is created, the adsorbate transitions to the TNI PES. The TNI PES typically has a different equilibrium bond distance compared to that of the ground state PES. As a result of the altered equilibrium bond distance, the adsorbate experiences acceleration along a particular nuclear degree of freedom. This acceleration results in either a chemical transformation on the TNI PES, or a gain in vibrational energy upon return to the electronic ground state PES, i.e. when the electron decays back to the metal, Figure 3c.[50,81−83] When the adsorbate returns to its electronic ground state PES in an excited vibrational state, the gained energy is dissipated through coupling to the metal surface over the course of 1−10 ps. The first order rate dependence on intensity indicates that vibrationally excited adsorbates that do not undergo a chemical transformation due to TNI formation dissipate the gained vibrational energy into the metal prior to subsequent electron scattering events. It is worth noting that a mechanism called electronic friction has been proposed for electron driven reactions at metal surfaces.[84] But, in the case of low intensity illumination in the linear rate dependence regime, this mechanism will not play a major role in driving chemistry because of the relatively low electronic temperature under solar intensity illumination.[85]

There are many different factors that impact the efficiency of the transient electron transfer for inducing a chemical transformation. The first factor is the probability of the electron transfer from the metal to the adsorbate, which is governed by the electron transfer coupling efficiency.[86] The second factor is how much energy gain is required to induce the chemical reaction, which is governed by the activation barrier for the reaction and the temperature of the system.[31] The system temperature plays a role in controlling the required energy gain for reaction based on the exponential increase in the population of higher energy vibrational states with temperature. Basically, if the temperature of a system is increased, molecules will populate vibrational states closer to the activation barrier threshold energy and will require less energy exchange from the electron scattering through the adsorbate to overcome the activation barrier. The third factor is the amount of energy the TNI process deposits into the molecule. The amount of energy gained through the TNI process is a function of the shapes of the ground state and TNI PESs, the lifetime of the electronic state, the congruence of the scattering electron energy and the unpopulated adsorbate energy level, and the temperature of the system.[87] Many of these factors are adsorbate dependent, such as the coupling efficiency, shape of the PESs, and the energy of the unpopulated adsorbate level. These characteristics could play a role in inducing unique selectivity compared to a pure thermal process, through favorable interactions of plasmon derived charge carriers with targeted adsorbates.

dx.doi.org/10.1021/cs400993w | ACS Catal. 2014, 4, 116−128

Before discussing the unique role of LSPR excitation in the linear electron driven mechanism, we will discuss the superlinear (Rate $\propto I^n$, $n > 1$) dependence of photocatalytic rate on intensity due to similarities between the mechanisms. Superlinear behavior has been observed for H-D formation from H_2 and D_2 dissociation on Au nanoparticles,[73] and for plasmon driven ethylene epoxidation on Ag nanocube clusters,[31] see Figure 3d. In both cases the rate exhibited a linear dependence on intensity at low photon intensities and a transition to superlinear behavior at higher intensity (>300 mW/cm^2 in the case of ethylene epoxidation on Ag). In the case of H-D formation on Au the superlinearity was attributed to nanoparticle heating, although no evidence was provided to substantiate this mechanism.[73] On the other hand, for ethylene epoxidation it was stated that the superlinear behavior could not be explained by a superposition of linear (1 photon process) and exponential (heating process) functions indicating that the mechanism was not based on nanoparticle heating. Further evidence that the superlinear transition was not thermally based was provided by the positive relationship between the measured KIE for ethylene epoxidation on Ag nanocube clusters and illumination intensity during the transition between the linear and super linear regimes.[31]

This transition from linear to superlinear behavior has previously been observed for CO and O_2 desorption from Pt surfaces at orders of magnitude higher photon intensities and has been explained previously in terms of the desorption induced by multiple electronic transitions (DIMET) model.[88] In the linear regime, DIET, molecules dissociate or desorb when a single electron scattering event deposits sufficient vibrational energy in the reaction coordinate. If the amount of energy deposited is insufficient to overcome the activation barrier, the adsorbate dissipates the excited vibrational energy, returning to the equilibrium thermal vibrational distribution before a subsequent scattering event. The transition to the superlinear regime occurs when the frequency of electron-molecule scattering events becomes sufficiently high, such that the time scale between subsequent electronic excitations of an adsorbate become shorter than the time scale for molecules to dissipate their gained vibrational energy, see Figure 3e.[36] In the super linear regime, each molecule that reacts has interacted with charge carriers deriving from more than one photon.

As mentioned above, the linear and superlinear relationships between rate and intensity have been observed on metal single crystal surfaces, albeit with lower quantum yields (number of molecules produced per photon) and at much higher illumination intensities (for the transition to super linear regime) compared to plasmonic nanostructures. For example, the observation of the transition from the linear to superlinear regime in O_2 dissociation (the rate limiting step in ethylene epoxidation) on Ag nanocube clusters occurred at 10^9 lower illumination intensity compared to O_2 desorption on a Pt single crystal.[31,88] The significant enhancements in photocatalytic efficiency of plasmonic nanostructures compared to single crystal surfaces has been proposed to be due to a combination of multiple factors. First, the absorption coefficient of plasmonic nanostructures is significantly enhanced compared to metal single crystals. Second, plasmonic nanoparticles selectively absorb resonant photons at their surfaces, and their length scale is similar to that of the mean free path of electrons in these materials, giving energetic electrons a high probability of interacting with adsorbates.[27] On the other hand, photon absorption by single crystals mostly occurs in the bulk, and the large thickness of these crystals suggests a significant fraction of charge carriers will never reach the surface of the crystal.[79] Third, collections and 3-D assemblies of plasmonic nanoparticles are known to have enhanced optical cross sections and selectively channel photon energies into small volumes, known as hot spots, where photocatalysis may be very efficient.[89] It is expected that hot spots will have very high rates of localized energetic electron generation and thus higher rates of direct plasmonic photocatalysis. Lastly, light absorption by adsorbate covered plasmonic nanostructures may have a higher cross section for direct charge injection into the adsorbate, compared to adsorbate covered single crystals, which could drive chemistry very efficiently. Individually these mechanisms have been discussed in various contexts, but a quantitative description of each of these effects in the context of direct plasmon driven photocatalysis has yet to be achieved.

In this section we have discussed the various macroscopically observable relationships between photon intensity and induced reaction rates and related these to microscopic reaction mechanisms. Observations of both the linear and the superlinear processes, particularly at intensities below where significant heating is expected to occur, are clear signatures of electron driven processes on the metal surface. Although, these intensity dependent relationships substantiate the electron-driven nature of the observed photocatalysis, they do not provide evidence that LSPR excitation is responsible for observed photocatalysis. Further evidence implicating LSPR excitation can be drawn from wavelength dependent photocatalytic measurements, which we will discuss in the next section.

5. PHOTON WAVELENGTH DEPENDENCE OF PLASMONIC PHOTOCATALYSIS

Wavelength dependent photocatalytic measurements have classically been used to relate photon absorption properties of photocatalysts to their performance. In addition, comparing the wavelength dependence of two different photocatalytic reactions (different bonds being activated in the rate or selectivity controlling steps) on the same photocatalyst provides information regarding the impact of the adsorbate on photocatalytic efficiency. In the context of electron driven reactions on metal surfaces, there are two primary mechanisms by which adsorbate-specific bond activation could be manifested in wavelength dependent photocatalytic measurements. In the first mechanism different reactions may have similar qualitative trends in wavelength dependent photocatalytic rate, but different magnitudes in efficiency.[87] This would suggest that the difference in photocatalytic efficiencies is due to adsorbate dependent efficiency in the electron scattering process, which could be due to any of the variables mentioned above (e.g., coupling efficiency, shape of the PESs, etc.). In the second mechanism, two reactions may display different qualitative trends or shapes of the wavelength dependent photocatalytic rates.[90] This difference would suggest that adsorbates are having an impact on the photon absorption event (adsorbate or adsorbate induced states are involved in the photon induced electronic transition) and that this unique photon absorption event is driving the chemistry. It is anticipated that if plasmon dephasing occurs through a direct charge injection into the adsorbate (rather than into the metal and subsequent transfer to the adsorbate) the wavelength dependence would resemble an overlap of the LSPR spectrum and the molecular resonance absorption spectrum.

dx.doi.org/10.1021/cs400993w | ACS Catal. 2014, 4, 116−128

Although, reports to date of wavelength dependent photocatalysis on plasmonic nanoparticles are sparse and cannot yet resolve the aforementioned adsorbate dependent effects, unresolved mechanistic issues may point toward plasmon excitations allowing targeted bond activation through both of the mechanisms mentioned above. The wavelength dependent rate of direct plasmonic photocatalysis has been measured for ethylene epoxidation on Ag nanocube clusters,[31] H-D formation on Au nanoparticles,[73] and Na desorption from Na clusters.[57] In the case of ethylene epoxidation, the photocatalytic rate of reaction was measured as a function of long pass filter energy. The derivative of this dependence was compared to the relative plasmon intensity, which was calculated as the overlap integral of the source intensity and the UV−vis spectrum of the Ag nanocube catalysts, providing a measure of the rate of plasmon excitation. The action spectrum, on a constant power basis, shows that there is a reasonable agreement between the wavelength dependence of the photocatalytic rate and the plasmon intensity, see Figure 4a.[31] Photocatalytic H-D formation on Au nanoparticles was also measured as a function of wavelength on a per power basis, showing a similar reasonable agreement between the absorption spectrum of the catalyst and the photocatalytic rate, see Figure 4b.[73] The Na desorption from Na clusters also displays a similar trend as the other two systems and was also measured on a constant intensity basis, see Figure 2a.[57] It is worth noting that these studies normalized the photocatalytic rate by power, although it may be useful to normalize based on number of photons to provide a measurement of the efficiency of a photon of a given energy for driving chemistry.

The similarity between the wavelength dependent rates of photocatalysis and absorption spectrum of the plasmonic photocatalysts provides strong evidence that LSPR excitation was responsible for the photocatalytic activity. Furthermore, combining these wavelength dependent results with a linear dependence of photocatalytic rate on intensity, as a few studies have done, indicates that the LSPR excitation is driving photocatalysis through an electronic (nonthermal) mechanism. But, these results do not help to clarify whether photocatalysis is driven by direct charge injection into adsorbate states, CID, or through the interaction of adsorbates with energetic electrons in the metal produced via Landau damping. Previous reports have shown that the formation of covalent bonds between plasmonic surfaces and adsorbates can induce shifts in plasmon energies that are attributed to the modification of the surface electronic structure near E_F, which is responsible for supporting oscillating surface plasmons.[91] Involving adsorbate states in plasmon oscillation and direct charge transfer may have an effect on photocatalysis, but the systems studied to date via wavelength dependent measurements focus on activation of weakly bound adsorbates (H_2 and O_2) and are not expected to show a significant deviation from the LSPR spectrum. Further investigations of direct plasmonic photocatalysis of strongly bound adsorbates that significantly perturb the plasmonic surface electronic structure may provide useful insight into the efficacy of CID for driving photocatalysis.

Wavelength dependent results have clearly provided convincing evidence in multiple cases that LSPR excitation was responsible for driving direct plasmonic photocatalysis. However, the limited number of experiments that have been performed preclude us from making definitive statements on whether charge injection into adsorbates occurs at the instant of plasmon dephasing or sometime after desphasing and the possible effectiveness of using LSPR excitations to modulate selectivity through adsorbate specific activation. Although more careful and expansive experimental measurements are expected to provide deeper insights into unanswered questions, theoretical treatments of direct plasmonic photocatalysis are also expected to play a role in answering fundamental questions; previously developed models will be discussed in the next section.

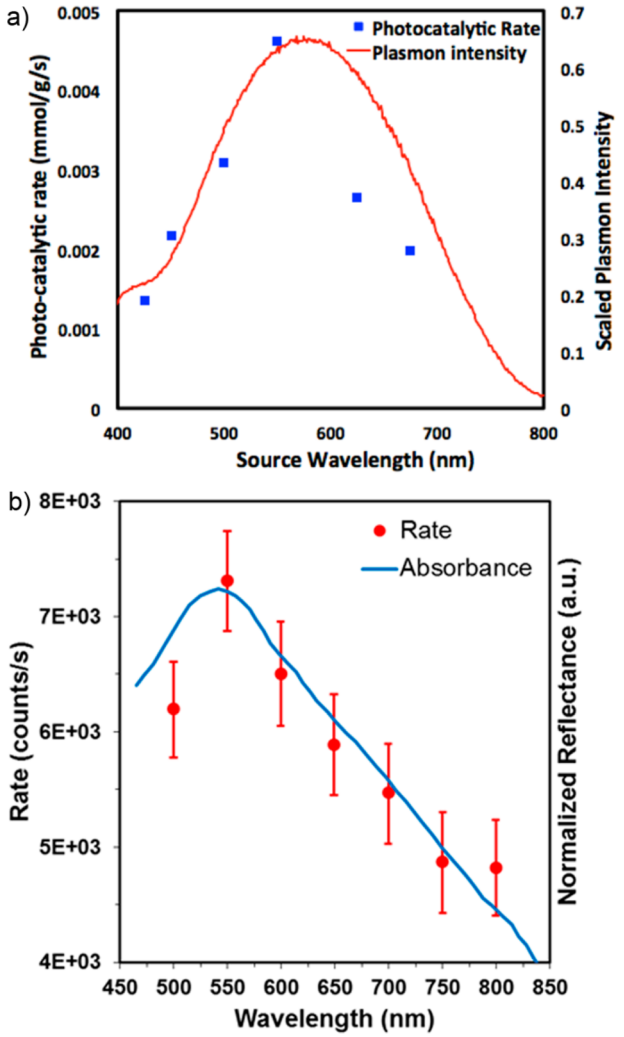

Figure 4. (a) Photocatalytic ethylene epoxidation rate on Ag nanocubes supported on Al_2O_3 (blue squares) and plasmon intensity spectrum (red line) measured as a function of illumination photon wavelength. Reproduced with permission from ref 31. Copyright 2012 Nature Publishing Group. (b) Photocatalytic rate of HD formation using Au nanoparticles supported on TiO_2 (red circles) and diffuse reflectance spectrum (blue line) measured as a function of wavelength. Modified from ref 73. Copyright 2012 American Chemical Society.

6. THEORETICAL DESCRIPTIONS OF DIRECT PLASMONIC PHOTOCATALYSIS

A thorough theoretical description of direct plasmonic photocatalysis requires spanning length and time scales from angstroms to hundreds of nanometers and femtoseconds to tens of picoseconds. This holistic picture is far from being achieved, but significant advances in modeling of various regimes of length and time have been developed and provide important insight into direct plasmon driven photocatalysis.

dx.doi.org/10.1021/cs400993w | ACS Catal. 2014, 4, 116−128

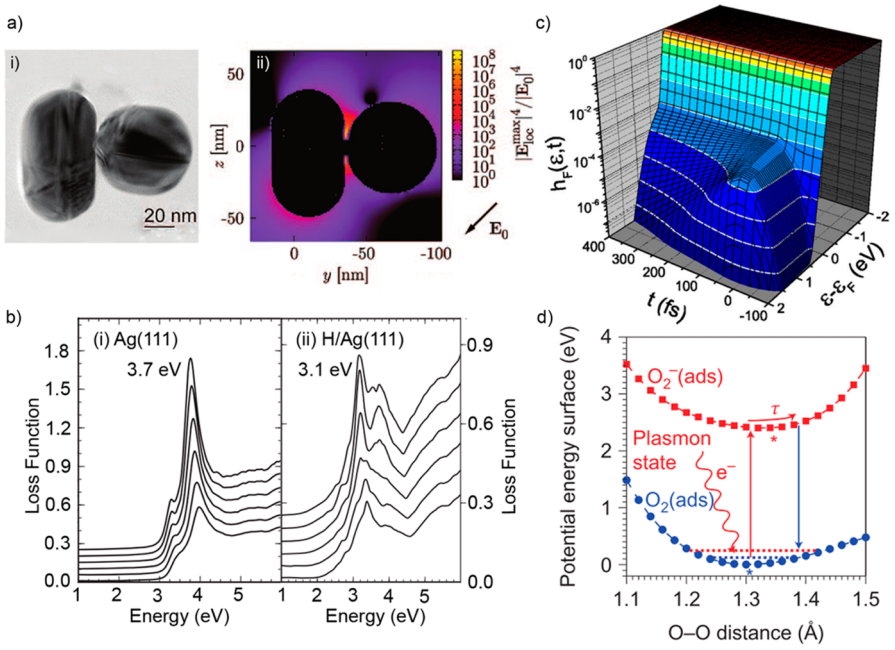

Figure 5. (a) (i) High Resolution transmission electron micrograph of a single-molecule SERS active Ag dimer and (ii) the calculated spatially dependent SERS enhancement of the same Ag dimer. Modified from ref 95. Copyright 2008 American Chemical Society. (b) Electron-energy-loss functions (analogous to absorption spectrums) calculated using TDDFT showing a peak at (i) ∼3.7 eV for Ag(111) and (ii) ∼3.1 eV for a Ag(111) surface coated with a monolayer of hydrogen. Modified from ref 48. Copyright 2011 American Physical Society. (c) Calculated time and energy dependence of the electron energy distribution (h_f) above E_f in a Au film following femtosecond laser excitation. Reproduced with permission from ref 99. Copyright 2006 American Physical Society. (d) Ground state and TNI PESs calculated from standard DFT and Δ SCF-DFT, respectively, for O_2 on Ag(100). Reproduced with permission from ref 43. Copyright 2011 Nature Publishing Group.

Following the physical phenomenon temporally, predictive theories of plasmonic photocatalysis must first describe the heterogeneously distributed electric fields on plasmonic photocatalysts as a function of photon excitation wavelength and intensity. The fastest time scale process occurring in parallel with plasmon excitation is the direct injection of electrons to adsorbates via CID.[92] Concurrently with and following CID, Landau damping produces a temporally evolving distribution of energetic electrons in the metal that could be interacting with adsorbates, during the first ∼1 ps after plasmon dephasing.[38] Finally this electronic energy will dissipate to heat, which should also be considered in the modeling of plasmonic photocatalysis.[38] We will discuss state-of-the-art theoretical treatments of each of these phenomena in the context of experimental validations.

Many of the plasmonic photocatalysts studied to date can be characterized as assemblies or collections of plasmonic nanoparticles randomly distributed on porous 3D oxides. Accurate descriptions of the distribution of electromagnetic fields in collections of particles will provide useful information about local rates of plasmon excitations and decay, which could then be related to photocatalytic activity. This requires the use of classical electromagnetic simulations in combination with quantum mechanical approaches to describe fields between plasmonic nanoparticles separated by less than 1−2 nm. Typically, electric field distributions are calculated using either the dynamic dipole approximation (DDA)[93] or finite-difference time-domain (FDTD) approach.[94] Although, hot spot identification and relation to photocatalysis has not been achieved, there have been many examples of correlated SERS studies where hot spots have been identified. For example, Figure 5a shows experimental and theoretical identification of an intersection between two Ag nanoparticles where single molecule SERS was achieved.[95] Also, recent approaches have been used to bridge classical and quantum mechanical interactions to more accurately describe energy exchange and field intensities at hot spots created by intersections of particles, which may also provide useful information for plasmon driven photocatalysis.[96−98] The execution of correlated photocatalytic experiments, where locations of highly active photocatalytic sites in 3D systems are related to their relationship to theoretical descriptions of electric field intensities, would provide very useful information for the design of optimized materials.

The question of how, or if, CID plays a role in driving direct plasmonic photocatalysis necessitates an understanding of how adsorbates impact or govern the electronic transitions occurring during plasmon oscillation as well as dephasing and whether these electronic transitions are related to photocatalysis. Experimentally, CID has been observed as a significant reduction in the dephasing time of small Au nanocrystals upon the addition of strongly bound adsorbates, such as SO_2 and thiols.[45,100,101] Theoretical descriptions of the impact of adsorbates on electronic transitions involved in plasmon excitations have recently been achieved using variations of TDDFT calculations.[48,102,103] For example, Yan et al. examined the impact of H adsorption on the excitation of plasmons on an Ag surface using linear response TDDFT.[48] It was shown that the adsorption of H onto Ag red-shifted the LSPR peak energy by 0.6 eV and that the red-shifted peak was primarily due to electronic transitions between H 1s states and Ag p states, see Figure 5b. This indicates that adsorbate electronic states can be involved in electronic transitions during plasmon excitation, which may provide a potentially useful route for adsorbate specific photoexcitation. Regardless of the initial evidence, theoretical treatments or experimental measurements of the

dx.doi.org/10.1021/cs400993w | ACS Catal. 2014, 4, 116−128

changes in electronic structure due to molecule adsorption on plasmonic surfaces have yet to be related to changes in dephasing time or photocatalytic functionality.

The process of Landau damping of the collective plasmon oscillations to form a single electron excitation and the exchange of energy between this excitation and other electrons and phonons after a pulsed laser excitation are well-established phenomena typically treated using the extended two-temperature model (ETTM). The ETTM takes into account electron−electron energy exchange through the Fermi-liquid approximation, which states that the rate of electron scattering (inversely proportional to the lifetime) is proportional to the square of the difference between the electron energy and the E_f.[39,99] Basically, the lifetime of energetic electrons above E_f decreases quadratically with increasing energy. The energy exchange between the energetic electrons and phonons is modeled using standard heat transfer approaches, where the rate of heat transferred is governed by the electron−phonon coupling constant. Using this approach, a temporally evolving electron energy distribution can be calculated following a pulsed photon excitation of a given intensity and wavelength, see Figure 5c.[99] Very recently Govorov et al. developed a self-consistent quantum mechanical description of the energetic electron distribution in plasmonic particles under continuous wave excitations.[104] This approach allows the calculation of steady-state energetic electron distribution in plasmonic nanoparticles as a function of size, shape, illumination intensity and wavelength, and local environments. These descriptions of the temporally evolving electron energy distribution after pulsed laser and during continuous wave excitations provide excellent starting points for the description and time scale of interactions between energetic electrons produced through Landau damping and unpopulated adsorbate states.

As stated earlier in the perspective, the efficiency of an electron scattering through an adsorbate orbital and subsequently driving chemistry depends upon a number of factors. An accurate description of the ground and TNI PESs would provide a majority of the important variables involved in the scattering process. Calculating ground state PESs for adsorbate transformations on surfaces can be achieved through well-established methods using ground-state DFT,[105] but obtaining accurate descriptions of TNI PESs is much more difficult. There are a number of methods that have been utilized to calculate TNI PESs of adsorbates on surfaces, such as TDDFT,[106] Δ self-consistent field theory DFT (Δ SCF-DFT),[107] and others.[108] These approaches have shown good accuracy in the calculation of resonance energies, (the energy required to move an electron from the metal into the unpopulated adsorbate state) for diatomic molecules on surfaces, but experimental validation of the shape of the excited state or TNI PESs have not been realized. An example of a ground state and TNI PES calculated for O_2 on Ag(100) using Δ SCF-DFT is shown in Figure 5d.[43] Furthermore, the ground state and TNI PESs have recently been used in the context of dynamic inelastic scattering models to calculate the impact of photon intensity, electron scattering rates, temperature, and isotopic labeling on the efficacy of plasmon driven photocatalysis.[31] The results of these simulations have shown excellent qualitative agreement with the various experimentally observed signatures of plasmonic photocatalysis discussed above. Based on the successful use of TNI PESs calculated from first principles to predict experimental signatures, we suggest that this approach could be used to examine the possibility of adsorbate specific excitation to manipulate selectivity in chemical transformations on plasmonic nanostructures.

These initial modeling efforts of various physical and chemical phenomena involved in direct plasmonic photocatalysis provide convincing evidence that the experimental observations can derive from electron driven processes. We expect that bringing these various phenomena together in multi scale models will begin to elucidate many of the unanswered questions regarding the mechanism and potential of direct plasmonic photocatalysis for manipulating reaction selectivity.

7. CONCLUSIONS AND OUTLOOK

Experimental and theoretical evidence for the utilization of LSPR excitations in the execution of electron-driven photocatalysis on plasmonic surfaces has become expansive over the past few years. A wide range of reactions have been demonstrated on Ag, Au, and Cu surfaces, showing that low intensity visible photon illumination can significantly enhance the rates of chemical transformations. In these processes, it is clear that LSPR excitations are focusing the energy of photons into enhancing the rate-limiting elementary steps in various chemical transformations. In addition to enhancing rates of chemical transformations on plasmonic nanostructure surfaces, a few cases have also emerged where LSPR excitation can be used to manipulate reaction selectivity, albeit with very different mechanisms.

Mechanistic studies have suggested that the majority of reported direct plasmonic photocatalysis occurs via the transient transfer of energetic electrons to adsorbate orbitals. In this process, adsorbates gain vibrational energy via vibronic energy exchanges that drive adsorbates over activation barriers. It has been proposed that the nature of the adsorbate may have a significant impact on the efficiency of this process, potentially allowing for a unique knob to control selectivity in plasmon driven reactions, although this has not yet been conclusively demonstrated. The development of relationships between adsorbate electronic structure and plasmonic photocatalytic signatures is of significant importance for designing plasmonic systems that allow for unique control of reaction selectivity.

Another area of research that has not yet emerged in direct plasmon driven photocatalysis is the development of structure−function relationships based on the size and shape of the plasmonic photocatalysis. An extremely well-known feature of plasmonic nanostructures is their tunable LSPR wavelength and primary plasmon decay mechanism with particle geometry. The dependence of direct plasmon driven photocatalytic characteristics (efficiencies, wavelength dependence, reaction selectivity, etc.) on the structure of the plasmonic nanoparticles is expected to be a focus of future research.

AUTHOR INFORMATION

Corresponding Author

*E-mail: christopher@engr.ucr.edu.

Author Contributions

P.C. is the Ph.D. adviser of M.J.K. and T.A.

Notes

The authors declare no competing financial interest.

ACKNOWLEDGMENTS

The authors thank the University of California, Riverside for funding and support.

REFERENCES

(1) Fujishima, A.; Honda, K. *Nature* **1972**, *238*, 37−38.
(2) Thampi, K. R.; Kiwi, J.; Grätzel, M. *Nature* **1987**, *327*, 506−508.
(3) Linsebigler, A.; Lu, G.; Yates, J. T. *Chem. Rev.* **1995**, *95*, 735−758.
(4) Kudo, A.; Miseki, Y. *Chem. Soc. Rev.* **2009**, *38*, 253−278.
(5) Mallouk, T. E. *J. Phys. Chem. Lett.* **2010**, *1*, 2738−2739.
(6) Roy, S. C.; Varghese, O. K.; Paulose, M.; Grimes, C. A. *ACS Nano* **2010**, *4*, 1259−1278.
(7) Dhakshinamoorthy, A.; Navalon, S.; Corma, A.; Garcia, H. *Energy Environ. Sci.* **2012**, *5*, 9217−9233.
(8) Maeda, K.; Teramura, K.; Lu, D.; Takata, T.; Saito, N.; Inoue, Y.; Domen, K. *Nature* **2006**, *440*, 295.
(9) Marimuthu, A.; Zhang, J.; Linic, S. *Science* **2013**, *339*, 1590−1593.
(10) Bonn, M.; Funk, S.; Hess, C.; Denzler, D. N.; Stampfl, C.; Scheffler, M.; Wolf, M.; Ertl, G. *Science* **1999**, *285*, 1042−1045.
(11) Bligaard, T.; Nørskov, J. K.; Dahl, S.; Matthiesen, J.; Christensen, C. H.; Sehested, J. *J. Catal.* **2004**, *224*, 206−217.
(12) Sabatier, P. *Ber. Dtsch. Chem. Ges.* **1911**, *44*, 1984−2001.
(13) Abild-Pedersen, F.; Greeley, J.; Studt, F.; Rossmeisl, J.; Munter, T.; Moses, P.; Skúlason, E.; Bligaard, T.; Nørskov, J. K. *Phys. Rev. Lett.* **2007**, *99*, 016105.
(14) Nørskov, J. K.; Bligaard, T.; Kleis, J. *Science* **2009**, *324*, 1655−1656.
(15) Freund, H.-J. *Top. Catal.* **2008**, *48*, 137−144.
(16) Somorjai, G. A.; Rioux, R. M. *Catal. Today* **2005**, *100*, 201−215.
(17) Christopher, P.; Ingram, D. B.; Linic, S. *J. Phys. Chem. C* **2010**, *114*, 9173−9177.
(18) Ingram, D.; Linic, S. *J. Am. Chem. Soc.* **2011**, *133*, 5202−5205.
(19) Zheng, Z.; Huang, B.; Qin, X.; Zhang, X.; Dai, Y.; Whangbo, M.-H. *J. Mater. Chem.* **2011**, *21*, 9079−9087.
(20) Wang, P.; Huang, B.; Qin, X.; Zhang, X.; Dai, Y.; Wei, J.; Whangbo, M.-H. *Angew. Chem., Int. Ed.* **2008**, *47*, 7931−7933.
(21) Mubeen, S.; Lee, J.; Singh, N.; Krämer, S.; Stucky, G. D.; Moskovits, M. *Nat. Nanotechnol.* **2013**, *8*, 247−251.
(22) Linic, S.; Christopher, P.; Xin, H.; Marimuthu, A. *Acc. Chem. Res.* **2013**, *46*, 1890−1899.
(23) Warren, S. C.; Thimsen, E. *Energy Environ. Sci.* **2012**, *5*, 5133−5146.
(24) Linic, S.; Christopher, P.; Ingram, D. B. *Nat. Mater.* **2011**, *10*, 911−921.
(25) Wang, P.; Huang, B.; Dai, Y.; Whangbo, M.-H. *Phys. Chem. Chem. Phys.* **2012**, *14*, 9813−9825.
(26) Nitzan, A.; Brus, L. E. *J. Chem. Phys.* **1981**, *75*, 2205−2214.
(27) Kreibig, U.; Vollmer, M. *Optical Properties of Metal Clusters*; Springer: Berlin, Germany, 1995.
(28) Chou, L.-W.; Shin, N.; Sivaram, S. V.; Filler, M. A. *J. Am. Chem. Soc.* **2012**, *134*, 16155−16158.
(29) Link, S.; El-Sayed, M. A. *Int. Rev. Phys. Chem.* **2000**, *19*, 409−453.
(30) Brus, L. *Acc. Chem. Res.* **2008**, *41*, 1742−1749.
(31) Christopher, P.; Xin, H.; Marimuthu, A.; Linic, S. *Nat. Mater.* **2012**, *11*, 1044−1050.
(32) Link, S.; El-Sayed, M. A. *J. Phys. Chem. B* **1999**, *103*, 4212−4217.
(33) Watanabe, K.; Menzel, D.; Nilius, N.; Freund, H.-J. *Chem. Rev.* **2006**, *106*, 4301−4320.
(34) Molina, R. A.; Weinmann, D.; Jalabert, R. A. *Phys. Rev. B* **2002**, *65*, 155427.
(35) Petek, H.; Ogawa, S. *Prog. Surf. Sci.* **1997**, *56*, 239−310.
(36) Ho, W. *J. Phys. Chem.* **1996**, *100*, 13050−13060.
(37) Moskovits, M. *Rev. Mod. Phys.* **1985**, *57*, 783−826.
(38) Guillon, C.; Langot, P.; Del Fatti, N.; Vallée, F. *Proc. SPIE* **2004**, *5352*, 65−76.
(39) Della Valle, G.; Conforti, M.; Longhi, S.; Cerullo, G.; Brida, D. *Phys. Rev. B* **2012**, *86*, 155139.
(40) Voisin, C.; Del Fatti, N.; Christofilos, D.; Vallée, F. *J. Phys. Chem. B* **2001**, *105*, 2264−2280.
(41) Zhu, X.-Y. *Surf. Sci. Rep.* **2004**, *56*, 1−83.
(42) Vallée, F. In *Non-Equilibrium Dynamics of Semiconductors and Nanostructures*; Tsen, K.-T., Ed.; Taylor & Francis Group: Boca Raton, FL, 2006; pp 101−142.
(43) Christopher, P.; Xin, H.; Linic, S. *Nat. Chem.* **2011**, *3*, 467−472.
(44) Govorov, A. O.; Richardson, H. H. *Nano Today* **2007**, *2*, 30−38.
(45) Hendrich, C.; Bosbach, J.; Stietz, F.; Hubenthal, F.; Vartanyan, T.; Träger, F. *Appl. Phys. B: Lasers Opt.* **2003**, *76*, 869−875.
(46) Persson, B. N. J. *Surf. Sci.* **1993**, *281*, 153−162.
(47) Charlé, K.-P.; Frank, F.; Schulze, W. *Ber. Bunsenges. Phys. Chem.* **1984**, *88*, 350−354.
(48) Yan, J.; Jacobsen, K. W.; Thygesen, K. S. *Phys. Rev. B* **2011**, *84*, 235430.
(49) *Laser Spectroscopy and Photochemistry on Metal Surfaces*; Dai, H.-L.; Ho, W., Eds.; World Scientific Publishing Co.: Singapore, 1995.
(50) Menzel, D. *J. Chem. Phys.* **2012**, *137*, 091702.
(51) Yates, J. T. *J. Chem. Phys.* **2012**, *137*, 091701.
(52) Suh, J. S.; Jang, N. H.; Jeong, D. H.; Moskovits, M. *J. Phys. Chem.* **1996**, *100*, 805−813.
(53) Sun, M.; Xu, H. *Small* **2012**, *8*, 2777−2786.
(54) Kim, K.; Kim, K. L.; Shin, K. S. *Langmuir* **2013**, *29*, 183−190.
(55) Campion, A.; Kambhampati, P. *Chem. Soc. Rev.* **1998**, *27*, 241−250.
(56) Otto, A. *J. Raman Spectrosc.* **1991**, *22*, 743−752.
(57) Hoheisel, W.; Jungmann, K.; Vollmer, M.; Weidenauer, R.; Träger, F. *Phys. Rev. Lett.* **1988**, *60*, 1649−1652.
(58) Kidd, R.; Meech, S.; Lennon, D. *Chem. Phys. Lett.* **1996**, *262*, 142−150.
(59) Kidd, R. T.; Lennon, D.; Meech, S. R. *J. Chem. Phys.* **2000**, *113*, 8276−8282.
(60) Chen, X.; Zhu, H.-Y.; Zhao, J.-C.; Zheng, Z.-F.; Gao, X.-P. *Angew. Chem.* **2008**, *47*, 5353−5356.
(61) Zhu, H.; Chen, X.; Zheng, Z.; Ke, X.; Jaatinen, E.; Zhao, J.; Guo, C.; Xie, T.; Wang, D. *Chem. Commun.* **2009**, *48*, 7524−7526.
(62) Chen, X.; Zheng, Z.; Ke, X.; Jaatinen, E.; Xie, T.; Wang, D.; Guo, C.; Zhao, J.; Zhu, H. *Green Chem.* **2010**, *12*, 414−419.
(63) Zhu, H.; Ke, X.; Yang, X.; Sarina, S.; Liu, H. *Angew. Chem.* **2010**, *49*, 9657−9661.
(64) Zhao, J.; Zheng, Z.; Bottle, S.; Chou, A.; Sarina, S.; Zhu, H. *Chem. Commun.* **2013**, *49*, 2676−2678.
(65) Ke, X.; Sarina, S.; Zhao, J.; Zhang, X.; Chang, J.; Zhu, H. *Chem. Commun.* **2012**, *48*, 3509−3511.
(66) González-Béjar, M.; Peters, K.; Hallett-Tapley, G. L.; Grenier, M.; Scaiano, J. C. *Chem. Commun.* **2013**, *49*, 1732−1734.
(67) Navalon, S.; de Miguel, M.; Martin, R.; Alvaro, M.; Garcia, H. *J. Am. Chem. Soc.* **2011**, *133*, 2218−2226.
(68) Wee, T.-L.; Schmidt, L. C.; Scaiano, J. C. *J. Phys. Chem. C* **2012**, *116*, 24373−24379.
(69) Sun, M.; Huang, Y.; Xia, L. *J. Phys. Chem. C* **2011**, *115*, 9629−9636.
(70) Chen, K.-H.; Pu, Y.-C.; Chang, K.-D.; Liang, Y.-F.; Liu, C.-M.; Yeh, J.-W.; Hsu, Y.-J. *J. Phys. Chem. C* **2012**, *116*, 19039−19045.
(71) Wang, F.; Li, C.; Chen, H.; Jiang, R.; Sun, L.-D.; Li, Q.; Wang, J.; Yu, J. C.; Yan, C.-H. *J. Am. Chem. Soc.* **2013**, *135*, 5588−5601.
(72) Sun, M.; Zhang, Z.; Kim, Z. H.; Zheng, H.; Xu, H. *Chem.—Eur. J.* **2013**, *19*, 14958−14962.
(73) Mukherjee, S.; Libisch, F.; Large, N.; Neumann, O.; Brown, L.; Cheng, J.; Lassiter, J. B.; Carter, E.; Nordlander, P.; Halas, N. *Nano Lett.* **2012**, *13*, 240−247.
(74) Wang, C.; Ranasingha, O.; Natesakhawat, S.; Ohodnicki, P. R.; Andio, M.; Lewis, J. P.; Matranga, C. *Nanoscale* **2013**, *5*, 6968−6974.
(75) Kim, K. H.; Watanabe, K.; Mulugeta, D.; Freund, H.-J.; Menzel, D. *Phys. Rev. Lett.* **2011**, *107*, 047401.
(76) Madey, T. E.; Yates, J. T.; King, D. A.; Uhlaner, C. J. *J. Chem. Phys.* **1970**, *52*, 5215−5220.
(77) Funk, S.; Bonn, M.; Denzler, D. N.; Hess, C.; Wolf, M.; Ertl, G. *J. Chem. Phys.* **2000**, *112*, 9888−9897.
(78) Denzler, D.; Frischkorn, C.; Hess, C.; Wolf, M.; Ertl, G. *Phys. Rev. Lett.* **2003**, *91*, 226102.

(79) Zhou, X.-L.; Zhu, X.-Y.; White, J. M. *Surf. Sci. Rep.* **1991**, *13*, 73−220.
(80) Zimmermann, F. M.; Ho, W. *Surf. Sci. Rep.* **1995**, *22*, 127−247.
(81) Ho, W. *Surf. Sci.* **1996**, *363*, 166−178.
(82) Gadzuk, J. W. *Chem. Phys.* **2000**, *251*, 87−97.
(83) Czyzewski, J. J.; Madey, T. E.; Yates, J. T. *Phys. Rev. Lett.* **1974**, *32*, 777−780.
(84) Brandbyge, M.; Hedegård, P.; Heinz, T. F.; Misewich, J. A.; Newns, D. M. *Phys. Rev. B* **1995**, *52*, 6042−6056.
(85) Petek, H. *J. Chem. Phys.* **2012**, *137*, 091704.
(86) Lindstrom, C. D.; Zhu, X.-Y. *Chem. Rev.* **2006**, *106*, 4281−4300.
(87) Olsen, T.; Gavnholt, J.; Schiøtz, J. *Phys. Rev. B* **2009**, *79*, 035403.
(88) Busch, D. G.; Ho, W. *Phys. Rev. Lett.* **1996**, *77*, 1338−1341.
(89) Michaels, A. M.; Brus, L. *J. Phys. Chem. B* **2000**, *104*, 11965−11971.
(90) Ying, Z.; Ho, W. *J. Chem. Phys.* **1991**, *94*, 5701−5714.
(91) Mulvaney, P. *Langmuir* **1996**, *12*, 788−800.
(92) Kreibig, U.; Bour, G.; Hilger, a.; Gartz, M. *Phys. Status Solidi* **1999**, *175*, 351−366.
(93) Draine, B. T.; Flatau, P. J. *J. Opt. Soc. Am. A* **1994**, *11*, 1491−1499.
(94) Taflove, A.; Brodwin, M. *IEEE Trans. Microwave Theory Tech.* **1975**, *23*, 623−630.
(95) Camden, J. P.; Dieringer, J. A.; Wang, Y.; Masiello, D. J.; Marks, L. D.; Schatz, G. C.; Van Duyne, R. P. *J. Am. Chem. Soc.* **2008**, *130*, 12616−12617.
(96) Esteban, R.; Borisov, A. G.; Nordlander, P.; Aizpurua, J. *Nat. Commun.* **2012**, *3*, 1−9.
(97) Kelly, K. L.; Coronado, E.; Zhao, L. L.; Schatz, G. C. *J. Phys. Chem. B* **2003**, *107*, 668−677.
(98) Hao, E.; Schatz, G. C. *J. Chem. Phys.* **2004**, *120*, 357−366.
(99) Carpene, E. *Phys. Rev. B* **2006**, *74*, 024301.
(100) Bauer, C.; Abid, J.-P.; Girault, H. H. *J. Phys. Chem. B* **2006**, *110*, 4519−4523.
(101) Garcia, M.; de la Venta, J.; Crespo, P.; LLopis, J.; Penadés, S.; Fernández, A.; Hernando, A. *Phys. Rev. B* **2005**, *72*, 241403.
(102) Zhao, L.-B.; Huang, Y.-F.; Liu, X.-M.; Anema, J. R.; Wu, D.-Y.; Ren, B.; Tian, Z.-Q. *Phys. Chem. Chem. Phys.* **2012**, *14*, 12919−12929.
(103) Zhu, M.; Aikens, C. M.; Hollander, F. J.; Schatz, G. C.; Jin, R. *J. Am. Chem. Soc.* **2008**, *130*, 5883−5885.
(104) Govorov, A. O.; Zhang, H.; Gun'ko, Y. K. *J. Phys. Chem. C* **2013**, *117*, 16616−16631.
(105) Hammer, B.; Nørskov, J. *Adv. Catal.* **2000**, *45*, 71−129.
(106) Gavnholt, J.; Rubio, A.; Olsen, T.; Thygesen, K.; Schiøtz, J. *Phys. Rev. B* **2009**, *79*, 195405.
(107) Gavnholt, J.; Olsen, T.; Engelund, M.; Schiøtz, J. *Phys. Rev. B* **2008**, *78*, 075441.
(108) Libisch, F.; Cheng, J.; Carter, E. A. *Z. Phys. Chem.* **2013**, *227* (11), 1455−1466.